Departement für Kleintiere, Abteilung Radio-Onkologie

der Vetsuisse-Fakultät Universität Zürich

Leitung Abteilung Radio-Onkologie: Prof. Dr. med. vet. Carla Rohrer Bley

Arbeit unter wissenschaftlicher Betreuung von
Prof. Dr. med. vet. Carla Rohrer Bley

Dynamic *in vivo* profiling of DNA damage and -repair after radiotherapy using canine patients as a model

Inaugural-Dissertation

zur Erlangung der Doktorwürde der
Vetsuisse-Fakultät Universität Zürich

vorgelegt von

Nadine Schulz

Tierärztin
Oberhausen, Deutschland

genehmigt auf Antrag von

Prof. Dr. med. vet. Carla Rohrer Bley, Referentin
Prof. Dr. med. vet. Hanspeter Nägeli, Korreferent

2017

Departement für Kleintiere, Abteilung Radio-Onkologie

der Vetsuisse-Fakultät Universität Zürich

Leitung Abteilung Radio-Onkologie: Prof. Dr. med. vet. Carla Rohrer Bley

Arbeit unter wissenschaftlicher Betreuung von
Prof. Dr. med. vet. Carla Rohrer Bley

Dynamic *in vivo* profiling of DNA damage and -repair after radiotherapy using canine patients as a model

Inaugural-Dissertation

zur Erlangung der Doktorwürde der
Vetsuisse-Fakultät Universität Zürich

vorgelegt von

Nadine Schulz

Tierärztin
Oberhausen, Deutschland

genehmigt auf Antrag von

Prof. Dr. med. vet. Carla Rohrer Bley, Referentin
Prof. Dr. med. vet. Hanspeter Nägeli, Korreferent

2017

INDEX

Zusammenfassung

Vetsuisse-Fakultät Universität Zürich 2017

Nadine Schulz

Departement für Kleintiere
Abteilung Radio-Onkologie
onkologie@vetclinics.uzh.ch
ehuber@vetclinics.uzh.ch

In vivo Charakterisierung der Dynamik von DNA-Schäden und deren Reparatur unter Radiotherapie an Hunden als Modell

Die Beobachtung von DNA-Schäden und DNA-Reparatur an durch Radiotherapie behandelten Zellen liefert Informationen über deren intrinsische Radiosensitivität.
Bisher verfügen wir über wenige Informationen über den zeitlichen Ablauf von DNA-Reparatur in Tumorzellen, die direkt aus Patienten gewonnen wurden. Somit wurden von Weichteilsarkomen (n=6) und malignen Melanomen (n=2) von 8 Hunden sowie mitbestrahlten Normalgeweben wiederholt Proben vor und nach Radiotherapie entnommen und auf die Kinetik von DNA-Schäden und deren Reparatur analysiert.
Die Resultate wurden mit einem mathematischen Modell für DNA-Schäden verglichen. Als Analysemethoden für die Kinetik der DNA-Schäden und Reparatur fanden der Comet-Assay und Immunhistochemie für γH2AX Anwendung. Der prozentuale Anteil von DNA im Kometenschweif erreichte sein Maximum 15-60 Minuten nach Bestrahlung mit einem schnellen Abfall 120 Minuten nach Bestrahlung.
Während die basalen γH2AX-foci in Tumorproben von Weichteilsarkomen (n=16), malignen Melanomen (n=19), Karzinomen (n=25) und malignen Lymphomen (n=23) sich einzig bei den Lymphomen unterschieden, bestätigte die Focibildung von γH2AX nach Bestrahlung die Ergebnisse der Comet-Assays. Die in vivo Daten der Sarkome deckten sich gut mit dem mathematischen 2-Pathway-Modell, was für die Melanomdaten nicht zutraf.
Zusammenfassend deutet die Arbeit darauf hin, dass DNA-Schäden und deren Reparatur sich mit einer minimalinvasiven Methode im zeitlichen Ablauf untersuchen lassen.

Stichwörter: *DNA-Schäden, DNA-Reparatur,* γH2AX-Foci, Comet-Assay, Radiotherapie

Summary

Vetsuisse Faculty University of Zurich 2017

Nadine Schulz

Department for Small Animals
Division of Radiation Oncology
onkologie@vetclinics.uzh.ch
ehuber@vetclinics.uzh.ch

Dynamic *in vivo* profiling of DNA damage and -repair after radiotherapy using canine patients as a model

Monitoring formation and repair of damage in a cell after radiotherapy represents a means to provide information on intrinsic radiosensitivity. Little is known about the time course of DNA damage response in tumors sampled from individual patients. DNA damage produced by therapeutic ionizing radiation with repeated *in vivo* sampling of canine tumors and co-irradiated normal tissue were evaluated in 8 dogs with either soft tissue sarcoma (n=6) or malignant melanoma (n=2). *In vivo* results were compared with a dynamic mathematical model for DNA damage formation and repair by a 2-pathway model. Kinetics of DNA damage and repair were assessed with comet assay and γH2AX immunohistochemistry. The %DNA in tail peaked at 15-60 minutes after irradiation with a rapid decrease at 120 minutes. While baseline levels of γH2AX-foci in tumor samples from 83 dogs (soft tissue sarcomas (n=16), malignant melanomas (n=19), carcinomas (n=25), malignant lymphomas (n=23)) only differed in lymphomas, the time courses of γH2AX-foci after therapeutic radiation paralleled the findings from the comet assay with a small time delay, with no influences of covariates. The evolutionary parameter search revealed a good fit of the 2-pathway model to *in vivo* data for sarcoma, but not for melanoma when fast and slow processes were included. We conclude that DNA repair can be quantitatively investigated not only by evaluating initial or residual damage, but also by following time courses of individual patients.

Keywords: DNA damage repair, γH2AX-foci, comet assay, radiation, 2-pathway repair model

Dynamic *in vivo* profiling of DNA damage and -repair after radiotherapy using canine patients as a model

Nadine Schulz[1], Hassan Chaachouay[1], Katarzyna J. Nytko[1], Malgorzata Roos[2], Rudolf M. Füchslin[3], Mathias S. Weyland[3], Franco Guscetti[4], Stephan Scheidegger[3], Carla Rohrer Bley[1*]

[1] Division of Radiation Oncology, Vetsuisse Faculty University of Zurich, CH-8057 Zurich, Switzerland

[2] Department of Biostatistics, Epidemiology Biostatistics and Prevention Institute, Faculty of Medicine, University of Zurich, CH-8001 Zurich, Switzerland

[3] ZHAW School of Engineering, Zurich University of Applied Sciences, CH-8400 Winterthur, Switzerland

[4]Institute of Veterinary Pathology, Vetsuisse Faculty University of Zurich, CH-8057 Zurich, Switzerland

*Corresponding Author

E-mail: crohrer@vetclinics.uzh.ch

Abstract

Time resolved data of DNA damage and -repair after radiotherapy elucidates the relation between damage, repair and cell survival. While well characterized *in vitro*, little is known about the time course of DNA damage response in tumors sampled from individual patients.

Kinetics of DNA damage after radiotherapy was assessed from 8 dogs with repeated *in vivo* sampling of tumor and co-irradiated normal tissue with comet assay and γH2AX immunohistochemistry. *In vivo* results were then compared (*in silico*) with a dynamic mathematical model for DNA damage formation and repair by a 2-pathway-model.

Maximum %DNA in tail was observed at 15-60 minutes after irradiation, with a rapid decrease. Time courses of γH2AX-foci paralleled these findings with a small time delay, not influenced by covariates. The evolutionary parameter search (based on %DNA in tail) revealed a good fit of the 2-pathway-model to *in vivo* data for sarcoma, but not melanoma when fast and slow processes were included. It was possible to follow dynamics of comet tail intensity and γH2AX-foci during a course of radiation using a minimally invasive approach, and to integrate resulting data into a dynamic mathematical model, hence DNA repair can be quantitatively investigated by following time courses of individual patients.

Short title: DNA damage repair after radiotherapy

Keywords: DNA damage repair, kinetics, γH2AX-foci, comet assay, dog, radiation, 2-pathway repair model

Introduction

Monitoring the formation of damage in a cell after radiotherapy (RT) and the evaluation of DNA repair markers may be a means to provide information on intrinsic radiosensitivity and radio-responsiveness [1-3]. Ionizing radiation used as a cancer treatment relies on the formation of direct DNA damage or on creating sufficient cellular damage leading to double strand breaks (DSBs), which in turn trigger the activation of cellular death pathways. Upon damage, the cells activate a DNA-damage response, consisting of various pathways which will sense the extent of damage and induce an effector pathway either leading to cell death, cell cycle arrest or DNA damage repair [4]. DNA damage detection from patient samples has been performed for various tumor groups irradiated *ex vivo*, resulting in robust correlations with radio-responsiveness as known from clinical behavior [2,5]. Furthermore, monitoring the responses towards damage formation and repair from individual tumors may offer a legitimate chance to monitor cancer treatment and even a possibility to predict clinical response to treatment [6,7]. This is thought to hold true even in spite of high inter-tumoral and inter-patient heterogeneity that is to be expected from patient samples [6,7].

While the time courses in responses to different DNA damaging agents have been characterized well in cultured tumor cells *in vitro*, little is known about the time course of DNA damage response in tumor and normal tissues sampled from individual tumor patients [2,5,6,8-10]. Specifically, actual time courses from patients undergoing radiation therapy are lacking. Time resolved data of DNA damage formation and repair can be used to elucidate the relation between DNA damage formation, repair and cell survival. It can be expected that e.g. a higher amount of DNA fragments in the tail of a comet assay or residual γH2AX-foci are an indication for a higher initial radiosensitivity.

The aim of this study was twofold: first, we wanted to use the minimally invasive sampling techniques (fine needle aspirates (FNAs)) and small biopsies for repeated *in vivo* patient

sampling and subsequent biostatistically quantify the amounts and time courses of DNA damage produced by therapeutic ionizing radiation. As a model, sampling was performed in canine tumor tissue as well as of co-irradiated normal tissue from patients undergoing treatment. In order to study DNA damage in samples of low cellularity, the comet assay [11-13] was used to detect DNA breaks at the level of individual cells in a rapid, sensitive and simple manner. To validate our data from the alkaline comet assay and to gain additional information, staining of phosphorylated H2AX (γH2AX) foci was performed in parallel at several time-points after treatment with RT [14]. Second, the clinical *in vivo* results were then compared (*in silico*) with a dynamic mathematical model for DNA damage formation and repair by a 2-pathway model. With the postulation of a second order decay (removal) of DNA fragments in the comet tail, the goal of the introduction of clinical patient data into such a tumor-patient model is to identify characteristic kinetic constants and delay times [15].

By integrating the repeated, minimally invasive *in vivo* measurements of clinical patients treated with RT into a mathematical model based data analysis, the potential of computer simulation of such time courses was strengthened. This in turn will allow its future use in a more comprehensive framework for the interpretation of obtained patient data and for guidance of therapy.

Results

Treatment courses were followed analyzing the comet tails (% of DNA in tail) at the chosen time-points at the first and before the second fraction of radiotherapy. In parallel to the DNA content in comet tails, γH2AX foci at the chosen time-points were evaluated in tumor and co-irradiated normal tissue and the influences of covariates are described. The resulting data was used to compute the median DNA fragments at every time point *in silico*. Additionally, by evaluating a set of untreated tumor samples, a rough quantification of the basal levels of γH2AX foci in canine tumors was established.

Patient, tumor and radiation dose characteristics

Complete datasets of 8 patients were available for repeated sampling. From the 8 dogs, 4 were female (2 spayed) and 4 were neutered males. The dogs were of various pure (n=5) and mixed breeds (n=3) and a total of 5 breeds were represented. The ages ranged from 8.17-13.67 years with a mean of 11.28 (± 1.63) years. The weight ranged from 11.00-38.50 kg, with a mean of 23.73 (± 8.51) kg. Tumor volumes ranged from 9.24 to 97.91 cm^3 with a mean of 27.43 cm^3 (± 29.33). Of the 8 cases, 6 tumors (75%) were histologically described as canine soft tissue sarcoma and 2 (25%) as malignant oral melanoma. Radiation therapy was applied in 5x6 Gy over 2.5 weeks in 7 patients and in 4x8 Gy in one patient (with malignant melanoma).

Comet assay: tail intensities (% DNA in tail) after radiotherapy in tumor samples

Compared to pre-treatment (T_0), the measured %DNA tail peaked at 15 to 60 minutes after RT. The maximum %DNA in tail was observed at 15-60 minutes after irradiation, with a rapid decrease at 120 minutes. The median tail intensities differed significantly up to and including the 60 minutes post treatment time point ($p \leq 0.001$). Afterwards, a rapid decrease

was found, already after 120 and 360 minutes, as well as before the second fraction, where median tail intensity was not significantly different from T_0 anymore. (Table 1 and Additional file 2)

Table 1: Differences of median tail intensity (% DNA in tail), comet assay (%; 95%CI).

T_0, T_{15}, T_{30}, etc. indicate the time-points in minutes after completion of radiation treatment

Time-points	Difference of % DNA in tail (95%CI)	p-value
$T_0 \rightarrow T_{15}$	10.80 (6.56 – 15.04)	p=0.001
$T_0 \rightarrow T_{30}$	11.24 (6.38 – 16.10)	p=0.001
$T_0 \rightarrow T_{60}$	7.11 (4.52 – 9.71)	p<0.001
$T_0 \rightarrow T_{120}$	2.47 (-1.41 – 6.36)	p=0.172
$T_0 \rightarrow T_{360}$	1.24 (-0.86 – 3.33)	p=0.185
$T_0 \rightarrow T_{\text{before 2nd fraction}}$	1.56 (-0.87 – 3.99)	p=0.168

γH2AX: number of positive cells and of foci per cell after radiotherapy in tumor samples

Samples from three time-points (T_0, T_{30}, T_{360}) of the included patients were analyzed for the number of positive cells (%), as well as foci/cell. Both the amounts of positive cells as well as the numbers of foci per cell at T_{30} and T_{360} were significantly different from those at T_0 ($p<0.001$ for positive cells; $p=0.002$ for foci/cell). As shown in Tables 2, both values had returned to baseline before the second fraction. The concurrently sampled co-irradiated normal tissue from the tumor patients followed the same pattern regarding the disappearance of foci (Fig 1).

Table 2a: Positive staining (%) for γH2AX-foci. T_0, T_{30}, T_{360}, etc. indicate the time-points in minutes after completion of radiation treatment

Time-points	Median γH2AX positive cells (%; 95%CI)	p-value, compared to T_0
T_0	24.35	
T_{30}	86.95 (73.15 – 100.74)	p<0.001
T_{360}	79.50 (63.31 – 95.68)	p<0.001
$T_{\text{before 2nd fraction}}$	22.5 (6.58 – 38.13)	p=0.764

Table 2b: Number of γH2AX-foci per positive cell. T_0, T_{30}, T_{360}, etc. indicate the time-points in minutes after completion of radiation treatment

Time-points	Median γH2AX-foci per nucleus (95%CI)	p-value, compared to T_0
T_0	2.41	
T_{30}	10.49 (8.44 –2.54)	p<0.001
T_{360}	5.00 (3.88 – 6.12)	p=0.002
$T_{\text{before 2nd fraction}}$	2.00 (1.56 – 2.44)	p=0.163

Figure 1: Time course of γH2AX immunohistochemical labeling in normal epithelium, soft tissue sarcoma and malignant melanoma. All tissues show low γH2AX reactivity before radiotherapy, high numbers of γH2AX positive cells and foci per cell at 30 minutes after radiotherapy and a decrease of the respective numbers at 360 minutes after radiotherapy. (RT = radiotherapy; bars: overview 20 μm, insert 15 μm)

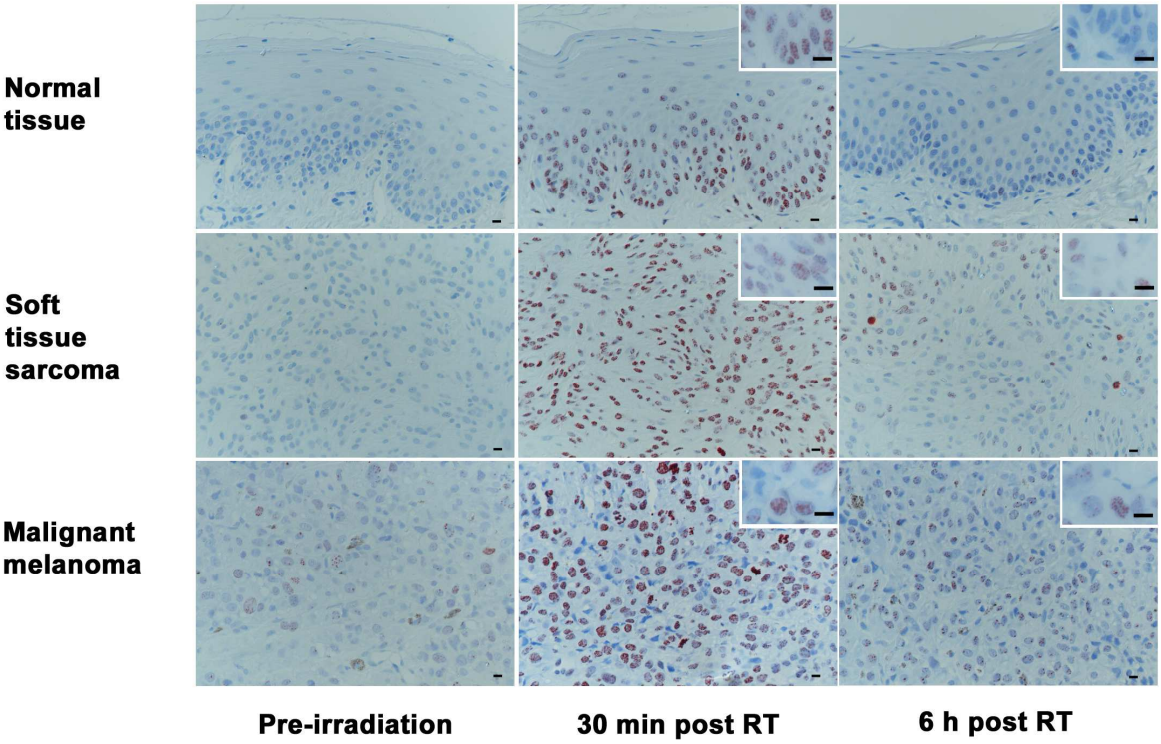

Covariate analysis

Due to the time dependence, a linear mixed model approach was applied to detect associations between the median tail intensity, median positive cells, median foci/cell and covariates such as age, gender, tumor volume and cancer type. No influence of the covariates or the different fractions of serial measurement was detected.

Baseline levels of γH2AX in tumor biopsy samples of various histologies

Samples of various histologies (soft tissue sarcomas (n=16), malignant melanomas (n=19), carcinomas (n= 25) and malignant lymphomas (n=23)) were taken from patients undergoing surgical tumor removal for diagnostic or treatment purposes at the clinic (see Table 3 for patient-specific details). While the sampling groups did not vary in gender (p=0.186), age (p=0.014, malignant lymphoma younger than malignant melanoma patients) and weight (p=0.016, soft tissue sarcomas heavier than malignant melanoma and carcinomas patients)

showed some (clinically non-relevant) differences. Histologically, the malignant lymphoma tumor group had significantly higher values in foci/cell ($p<0.001$), compared to the population with soft tissue sarcoma, malignant melanoma or carcinomas (Fig 2). For positive cells ($p=0.014$) the malignant lymphoma tumor group had significantly higher values than the population with soft tissue sarcoma.

Table 3: Patient specific details for baseline values of γH2AX foci. f= female, fs = female spayed, m = male, mn = male neutered

	Age [years] mean (SD; range)	**Weight** [kg] mean (SD; range)	**Gender**	**Median positive cells (%)**	**95% CI**	**p-value**	**Median foci / tumor**	**95% CI**	**p-value**
Overall (n=83)	9.89 (±2.92; 1.00-15.00)	23.70 (±10.90; 3.60-55.00)	f=14 fs=27 m=19 mn=23	20.72	21.88-24.29	0.014	2.50	2.40-2.90	<0.001
Soft tissue sarcoma (n=16)	9.74 (±1.80; 5.92-12.83	30.40 (±9.88; 14.20-50.70)	f=3 fs=7 m=3 mn=3	13.41	7.42-20.59		2.00	1.50-2.47	
Malignant melanoma (n=19)	11.71 (±2.59; 6.00-15.00)	19.24 (±8.78; 3.60-30.50)	f=2 fs=4 m=7 mn=6	15.35	12.25-28.22		2.50	2.14-2.99	
Carcinoma (n=25)	9.48 (±3.33; 1.00-15.00)	20.79 (±10.23; 4.50-35.50)	f=6 fs=6 m=8 mn=5	18.12	14.55-28.67		2.00	2.03-2.81	
Malignant lymphoma (n=23)	8.94 (±2.67; 3.58-13.75)	25.88 (±11.04; 9.00-55.00)	f=3 fs=10 m=1 mn=9	31.30	24.72-34.93		3.00	2.87-4.04	

Figure 2: Examples of baseline levels γH2AX immunohistochemical labeling in indicated tumor types. (Bars: overview 20 µm, insert 15 µm)

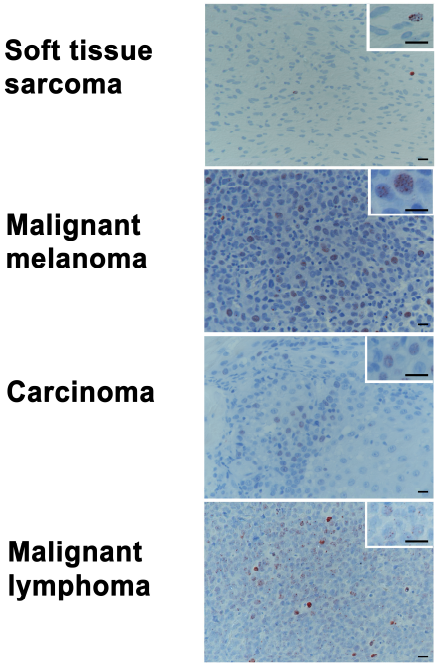

Quantification of the time course of DNA damage and –repair using novel mathematical modeling

The evolutionary parameter search (based on the median % DNA in tail) reveals a good fit to the *in vivo* data for the sarcoma when both processes (fast and slow) are included. Since in this data no shoulder is visible (neither in the average of 3 fractions nor in of the fractions), we tested the case when only the fast pathway is activated. This fit has a larger error (Table 4) but in relation to the scatter of the data (Fig 3a) it covers the experimental results fairly well. The melanoma data exhibit a shoulder, which is not very pronounced in the average of all fractions (Fig 3b), but is well visible in the comet data of the second fraction (Fig 3c and 3d). As shown in Fig 3c, the evolutionary parameter search fails to find parameters that represent the shoulder.

Table 4: Parameter sets of the bio-mathematical model for sarcoma and melanoma. For the final repair step, second order kinetics is assumed and the data is given in % DNA. The numbers given in parentheses in column 1 (sarcoma, average 3 fractions) are for a fit of the full model; for the other values in that column, it was assumed that the comet data are dominated by the fast process, since no shoulder is visible in the data.

Parameter	Sarcoma, average over 3 fractions	Melanoma, average over 2 fractions	Melanoma, 2nd fraction, best fit	Melanoma, 2nd fraction, hand-picked solution
k_{decay} / min^{-1}	1.93 (1.96)	1.93 (1.96)	2.69	3.56
$k_{0,fast}$ / min^{-1}	$3.93 \cdot 10^{-1}$ ($1.59 \cdot 10^{-1}$)	$3.93 \cdot 10^{-1}$ ($1.59 \cdot 10^{-1}$)	$9.69 \cdot 10^{-3}$	$8.75 \cdot 10^{-1}$
$k_{1,fast}$ / min^{-1}	$2.92 \cdot 10^{-2}$ ($3.44 \cdot 10^{-2}$)	$2.92 \cdot 10^{-2}$ ($3.44 \cdot 10^{-2}$)	$2.13 \cdot 10^{-3}$	$5.87 \cdot 10^{-2}$
$k_{2,fast}$ / min^{-1}	$1.00 \cdot 10^{-2}$ ($9.01 \cdot 10^{-3}$)	$1.00 \cdot 10^{-2}$ ($9.01 \cdot 10^{-3}$)	$2.82 \cdot 10^{1}$	$2.74 \cdot 10^{1}$
$k_{0,slow}$ / min^{-1}	- ($3.22 \cdot 10^{-3}$)	($3.22 \cdot 10^{-3}$)	$3.00 \cdot 10^{1}$	$7.59 \cdot 10^{-1}$
$k_{1,slow}$ / min^{-1}	- ($1.01 \cdot 10^{-3}$)	($1.01 \cdot 10^{-3}$)	$1.57 \cdot 10^{-2}$	$7.48 \cdot 10^{-3}$
$k_{2,slow}$ / min^{-1}	- ($1.23 \cdot 10^{2}$)	($1.23 \cdot 10^{2}$)	6.38	$4.22 \cdot 10^{1}$
$t_{r,slow}$ / min	- (7.07)	(7.07)	1.03	$5.34 \cdot 10^{1}$
$t_{r,fast}$ / min	$1.28 \cdot 10^{1}$ ($1.09 \cdot 10^{1}$)	$1.28 \cdot 10^{1}$ ($1.09 \cdot 10^{1}$)	$6.98 \cdot 10^{-1}$	6.38

b_n / % DNA	4.23 (4.09)	4.23 (4.09)	6.93	5.28
Error of fit	1.20 (1.03)	1.20 (1.03)	$1.50 \cdot 10^1$	$1.63 \cdot 10^1$

Figure 3: Time resolved comet data fitted by the bio-mathematical 2-pathway model. (a) Average of median % DNA in tail over 3 fractions for sarcoma cells, with only the fast repair pathway activated; (b) average of median % DNA in tail over 3 fractions for melanoma cells; (c) median % DNA in tail for 2nd fraction for melanoma cells with the parameters yielding the smallest error of fit; (d) median % DNA in tail for 2nd fraction for melanoma cells with a hand-picked solution representing the shoulder well at the expense of a larger error of fit; the error bars indicate the upper and lower quartile.

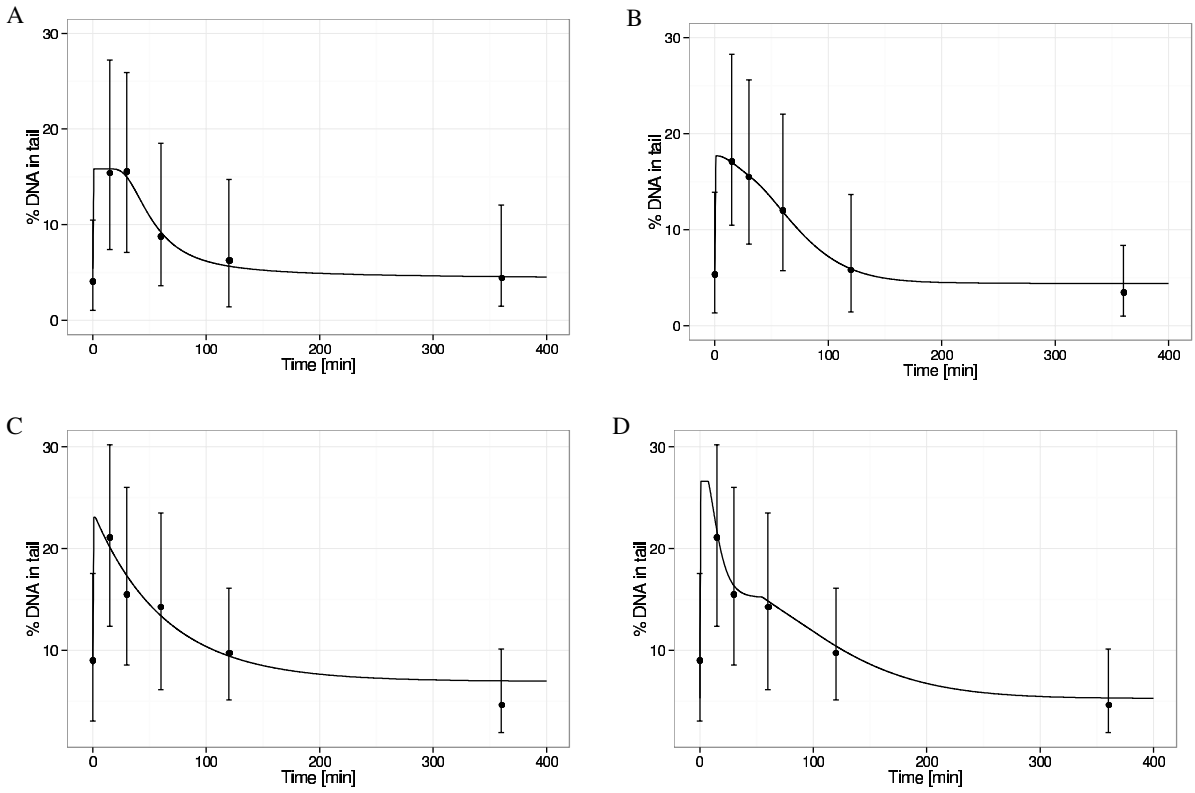

One of the possible reasons for this discrepancy between the *in vivo* data and the data generated by the model with the best fit according to the parameter search is as follows: The initial value (9.0% DNAin tail) before radiation is higher than the value at 360 min (4.6 % DNA in tail). Therefore, there are two baselines, one before and one after radiation. Since the model assumes one single baseline value, the error of fit remains large. As shown in Fig 4d, a hand-picked set of parameters does reproduce the shoulder at the expense of a slightly larger error of fit. The different parameter search runs reveal for some parameter varying values (especially $k_{2,fast}$) whereas other values seem to evolve to stable values (e.g. k_{cleav}, $t_{r,fast}$).

In diagrams in Fig 4, the inter-quartile distances indicate the inhomogeneity of the cells. Especially for melanoma cells, first and second fractions differ remarkably, whereas for sarcoma, the three fractions exhibit more or less the same shape of the curve (as shown in Fig. 4a, after a rise follows a decay as a result of first and second order processes).

Discussion

Up to date, to the author's knowledge, no DNA damage induction, or repair time-courses have been described from patients undergoing radiation therapy. Hence, very little is known about the amount of actual DNA damage and the kinetics of repair in tumors *in vivo*, as well as of normal tissues under antineoplastic treatment. Herein, we used repeated samples from dogs with primary tumors undergoing therapeutic radiation therapy. Spontaneous tumors in companion animals like dogs have been described to offer a unique opportunity as a model for human cancer biology and translational clinical research [15,16]. In contrast to most murine tumor xenograft studies, cancers in dogs arise over the background of an intact immune system and present many features like histological appearance, tumor genetics, molecular targets, biological behavior and response to conventional therapies, as well as inter-patient tumoral heterogeneity common to humans [15]. Moreover, in many terms a canine model will even serve better than the murine one to study DDR and its defects *in vivo,* as in rodents certain repair pathways seem to be less active in comparison to the human mechanisms, displaying a potentially a different emphasis and hierarchy of DNA repair pathways [17].

The intrinsic radiosensitivity of the tumor cells is a major determinant of the treatment response and outcome and correlates with patient's prognosis [18]. As summarized by McKenna et al., also the comet assay technique has been used in a wide range of human tumor cell lines as well as tissue biopsies and has shown predictive information value of the individual's sensitivity towards DNA damaging agents [13]. In this study, the kinetic median tail intensity (% DNA in tail) showed a fast time-course, with no significant remaining differences in tail intensity after 120 minutes post radiation for both soft tissue sarcoma as well as malignant melanoma samples. The alkaline comet assay was chosen because it is capable of detecting and quantifying effects of low, yet clinically relevant radiation doses of

0-6 Gy. Under alkaline conditions, DNA is denatured and both single strand breaks as well as double strand breaks are measured in the tail. In samples of human bladder cancer tissue irradiated *ex vivo*, evaluation for radiation induced DNA damage levels were measured by this method and the extent of comet formation was found to correlate with cell killing. Furthermore, in this patient cohort, reduced DNA damage sensitivity was associated with poorer treatment outcomes, implying a clinical predictive potential for treatment-induced DNA damage detection with the alkaline comet assay in certain tumors [6,19,20]. However, the alkaline comet assays is detecting both, double - and single strand breaks [21,22]. Hence, this assay is also detecting damage not necessarily directly responsible for cell death, as lethality is most frequently observed after non- or miss-repaired DSB. The neutral comet assay on the other hand can be modified to detect double strand breaks only, but this requires doses of radiation far higher than the clinically relevant ones. As a general advantage, comet assay is a relatively inexpensive, simple and fast technique that can be carried out on single-cell suspensions, requiring a small number of cells [13]. This in contrast to the more widely used clonogenic cell survival assay, which measures a surviving fraction of tumor cells after a given clinically relevant dose, but takes a number of weeks to be completed, e.g. to obtain the results of clonogenicity of the tumor cells [23]. Showing a strong correlation between the methods of clonogenic survival and alkaline comet assay at clinically relevant doses in tumor cell lines, these measurements of initial as well as residual DNA damage can probably be used to predict radiation sensitivity in patient derived tumor cells as well [19,20,24].

Prior work including *in vivo* mouse assays with various cell lines of head and neck carcinoma, as well as in *ex vivo* assays using different tumor types from patients has documented radio-responsiveness in sensitive and resistant tumor types to be represented by residual γH2AX-foci [1,2,5]. After antineoplastic treatment, the initiation of DNA repair by the two major responsible pathways is triggered by the phosphorylation of the histone protein H2AX that

leads to formation of γH2AX-molecules at the site of the DSB [4,25,26]. Upon repair, the γH2AX-foci will disappear over a time course, mostly in concert with DSB rejoining, but it is also suggested that a part of foci removal depends on subsequent steps of DSB rejoining [25,27]. Several reports describe the induction and decline of γH2AX foci *in vitro* [28-31], and also in cancer and normal tissues irradiated *in/ex vivo* [2,5,32,33]. It has been reported that γH2AX foci number in bone marrow cells of mice irradiated with 4 Gy peaked at 1 hour after treatment and decreased to baseline already after 4 hours, while in contrast γH2AX foci were still present in irradiated spermatocytes and round spermatid after 48 hours [33]. The kinetics of foci induction and disappearance depends on dose of ionizing radiation, intrinsic cellular radiosensitivity, cell cycle position and DNA content, the baseline levels of γH2AX and furthermore on microenvironmental conditions such as tissue oxygen concentration [34]. In accordance with our observations there is a general pattern of acute increase right after irradiation (5-30 minutes) with decrease between 0.5-24 hours after irradiation, depending on the type of tissue or cells [35]. As a common finding in cultured cancer cells as well as in malignant human tumors of different origins, also untreated canine cancers contain elevated levels of spontaneous γH2AX-foci, which are thought to represent inherent genomic instability [30]. The overall median number of 2.5 foci per cell found herein, ranging from 1.5-2.5 in soft tissue sarcomas to 2.9-4 in malignant lymphoma (e.g. high-grade non-Hodgkin's lymphoma) was within the range of 1-20 foci per cell described in human cancers and various canine cell lines [30,36]. In line with our data, recent reports show continuous activation of DNA-repair pathways and constitutive expression of γH2AX in human diffuse large B-cell lymphoma [28,37].

The bio-mathematical model chosen can be used to describe the comet assay derived-data for sarcoma, even when only one pathway is assumed to be activated. For melanoma data, the different baseline prior and after radiation caused problems for fitting: the lower baseline for

DNA fragments in tail after radiation may be a result of induced repair, which is not (yet) implemented in the bio-mathematical model. The evolutionary parameter search seems to be very sensitive to the constraints set for the optimization runs. In contrast to other models [38,39], the 2-pathway model used in this work summarizes the different process steps in a repair pathway by a delayed process. The consequence of this approach is on one hand a reduction of parameters but on the other hand a model containing Delay Differential Equations (DDE) which makes the evolutionary parameter search more difficult. The interpretation of the parameter values derived by fitting the comet data in this work remains challenging at this point. A better aggregation of the parameter values may be reached (1) by fitting data from more fractions and tumors and (2) by improving time resolution (especially time point 240 minutes and more time points in the shoulder region 10 - 120 minutes). The comparison with time-resolved γH2AX foci signals may be another option: however, the decay of γH2AX foci is slower (possibly due to the remaining of attached ATM after DNA strands are glued together) and therefore could mask the real dynamics of repair (e.g. the time course of DSB elimination)[40]. For gaining deeper insight into the full dynamics of the involved repair processes, dose-rate dependent data would be needed, representing a general limitation of using material from patients with spontaneous tumors. A full thorough characterization is more difficult compared to well-defined cell lines treated *in vitro*.

In this study, after a first data screening, we decided to group the data of sarcoma and melanoma patients for the initial modeling. One has to keep in mind that differences in intrinsic radiosensitivity in tumors of the same histological origin exist and can be remarkable [30,41,42]. As a further general limitation of this *in vivo* approach, minimally invasive and repetitive tumor sampling bears the risk of a mis-representation of the whole tumor due to intra-tumoral heterogeneity in the extent and distribution of malignancy, stromal reaction, inflammatory cells, necrosis and hypoxia. The sampling heterogeneity with fine needle

aspirates and subsequent comet assay might falsely reflect the intrinsic radiosensitivity or repair capacity, and the manipulation of single tumor cells and tissues can induce further sampling error. Sanguineous contamination may occur, leading to measurement errors with very high DNA intensities in the comet tail, an intensity error that can also be produced by early apoptotic cells [13,43]. Concurrent microscopic evaluations of FNA samples are recommended to assess the representativeness of a sample. These limitations however, reflect the clinical situation in any predictive testing for individual patients with the goal of personalized medicine and cannot be completely circumvented. However, in patient sample dependent mathematical data modeling they can be in part attenuated by choosing a high time resolution and large individual sample size.

At early time-points after RT, quantification of γH2AX foci was impaired due to foci overlap. However, this is a phenomenon also problematic for immunofluorescent staining and computerized quantification. In our evaluation, samples with foci numbers higher than 10 were adjusted as “25 foci” per cell. This was the case in samples taken 30 minutes and 6 hours after irradiation. Furthermore, there is an ongoing debate in the literature regarding what should be considered as focus, which is also subdued to certain subjectivity in manual scoring [44].

In conclusion, we confirm the clinical feasibility of repeated *in vivo* minimally invasive sampling with FNA as well as small biopsies in order to quantify the amounts and time courses of DNA damage produced by therapeutic RT. Both, dynamics of comet tail intensity and γH2AX-foci could be tracked during a course of radiation and the resulting data could be integrated into a dynamic mathematical model for DNA damage formation and repair by a 2-pathway model. By evaluating not only initial or residual DNA damage, but following a time course of an individual patient, DNA repair can be quantitatively described. The inclusion of individual patient measurement data into mathematical based model analysis can indicate the

types of repair predominating in this patient, leading to information that could impact the future practice of radiation therapy towards a personalized approach.

Materials and Methods

The current investigation involved samples of canine tumor patients with various types of cancers. In repeated samples from patients treated with RT, DNA damage formation and repair was assessed with comet assay (an assay used to investigate DNA damage in human biomonitoring and genotoxicology) [11-13] and γH2AX immunohistochemistry (representing an early event after double-strand break formation) [14,45] at defined time points. The resulting findings were then integrated into the bio-mathematical repair-pathway model in order to perform a model-based analysis of comet data. Additionally, biopsies of various tumors were screened with immunohistochemistry for the amount of pre-treatment γH2AX levels in order to define a baseline of DNA damage in canine tumors.

Patients and sampling procedures

Dogs presented to the Division of Radiation Oncology, Vetsuisse Faculty, University of Zurich, Switzerland for treatment of bulky malignant tumors between March 2014 and December 2015 were included into the study. Each dog had a clinical work up (tumor staging) as appropriate to the type of presenting disease. Written owner's consent was obtained for invasive sampling in this study. This study was carried out in strict accordance with the recommendations and the protocol approved by the Animal Ethics Council of the Canton of Zurich, Switzerland (Permit Numbers: 180/2011 and ZH108/15). All invasive sampling procedures were performed under anesthesia, and all efforts were made to minimize suffering. In addition, in order to investigate the basal level of γH2AX, a series of tumor biopsy samples of various histologies (soft tissue sarcomas, malignant melanomas, carcinomas and lymphomas) were taken from patients undergoing surgical tumor removal for diagnostic or treatment purposes at the clinic.

For comet assay analysis, tumor cells were collected with a minimally invasive method using fine-needle aspiration (FNA): Sampling was performed with a 5 ml syringe attached to a 22-gauge needle as described before [46]. The aspirated volume of 10 µl was immediately mixed with a freezing solution of 440 µl FCS and 50 µl DMSO in pre-cooled cryotubes. Cryotubes were stored at -80°C until comet assay was performed. FNA samples from the tumor site were taken in duplicates 15 minutes before RT and 15, 30, 60, 120 minutes and 6 hours after RT during the first and second fraction of radiotherapy.

Tumor biopsies were collected using 12-gauge Bard® Biopty-Cut® Disposable Core Biopsy Needles, and normal, co-irradiated tissue was sampled with 4 mm punches. Tissue was fixed for 24 h in 10% buffered formalin and embedded into paraffin wax by routine methods. Samples were taken 15 minutes before, 30 minutes and 6 hours after RT treatment.

Treatment

Radiation was delivered with a 6 megavolt (MV) linear accelerator (Clinac iX, Varian, Palo Alto, USA) using either photons or electrons, depending on tumor size and location. Treatment planning was performed on the basis of CT for photon plans or by hand calculation for electron plans. During treatment, dogs were under general anesthesia using propofol for induction- and sevoflurane for maintenance of anesthesia, immobilized in an individually shaped vacuum cushion and if required, additionally equipped with a custom-made bite block. The recommendations for specifying dose and volumes as proposed for veterinary medicine were adhered to as proposed in the corresponding literature. The prescribed dose was 30 Gy, delivered in 5 fractions of 6 Gy applied twice per week, resulting in an overall treatment time of 2.5 weeks [47-49].

Alkaline Comet Assay

After thawing, the FNA samples were mixed with 9 ml of ice-cold PBS and centrifuged for 10 min (1500 rpm, 4°C). The pellet was resuspended in 100 µl of ice-cold PBS. A volume corresponding to approximately 170'000 cells was mixed with 90 µl of agarose (1% LMPA in PBS, 37°C). Subsequently, 25 µl of agarose-cell solution was pipetted onto 20-well slides (Trevigen) in duplicate. The loaded slides were then placed at 4°C for 5 min to allow agarose polymerization, and subsequently placed in lysis buffer for 1 h at 4°C, followed by incubation twice in ice-cold alkaline electrophoresis solution (pH>13.0) for 10 min at 4°C in the dark. After electrophoresis (300 mA, 15 - 20 min), the slides were incubated twice for 10 min in dH_2O at room temperature followed by incubation in 70% ethanol for 5 min at room temperature in the dark. After complete drying, 70 µl of diluted SYBR-Green (1:10 000 in TE, pH8) was pipetted on every well and the slides were incubated for 15 min in the dark. The slides were washed twice for 10 min in dH_2O at room temperature. To provide a quantitative analysis of obtained comets (% DNA in tail, tail intensity), the COMET IV® scoring system was used.

γH2AX immunohistochemistry

Information about antibodies, pretreatment, incubation conditions and visualization are reported in Table 5. For immunohistochemical staining a Dako Autostainer (Dako, CH-6341 Baar) was used. Three µm sections were mounted on positively charged slides (Superfrost Plus), dried overnight at 37°C, deparaffinized, rehydrated and immersed for 10 min in 10% hydrogen peroxide to block endogenous peroxidase activity. Antibody diluent (S2022) and wash buffer (S3006) from Dako were used. Negative controls were done omitting the primary antibody.

Table 5: Antibodies and incubation conditions. Primary antibody, treatment and incubation conditions, *HIER= heat-induced epitope retrieval, carried out in a steamer (Pascal S2800, Dako)

Antigen	Vendor	Antibody Type	Catalogue no. / Clone	Dilution, Incubation Conditions	Pre-treatment	Visualsation Method	Positive Control
γH2AX Ser 139	Millipore	mouse mAb, IgG1	05-0636/clone JBW301	1:200, 1.3h, room temperature	HIER*, 20 min 98°C, citrate buffer pH 6.0	Envision Kit (Dako)	Irradiated canine tumor tissue

The quantification of γH2AX positively stained cells and γH2AX foci was performed by manual counting by one investigator (NS), after reaching internal consensus on the procedure. The tumor slides were scanned and analyzed with NanoZoomer 2.0-HT scanscope (Hamamatsu, CH-4500 Solothurn) and visualized using the NDP.view2 software (Hamamatsu). For each tumor 10 fields of identical size (50x magnification) were set randomly, but dispersed over non-necrotic tumor areas. Furthermore, in each tumor the number of γH2AX foci were counted in the nuclei of 300 cells.

Bio-mathematical modeling

For the bio-mathematical model, the following assumptions were made: DNA breaks can be processed by (1) a fast repair pathway reflecting Non-Homologues End-Joining (NHEJ) for DSB or SSB-repair by PARP-1/XRCC1/DNA repair module (which may be also involved in the DSB repair by the B-NHEJ backup pathway [50]) or by (2) a slower repair pathway (Homologous Recombination (HR) for DSB). Since SSB becomes also observable in an alkaline comet assay, it can be expected that DNA-fragments produced by direct DSB will be flanked by those initially produced by SSB. At this point it is not possible to relate a specific repair pathway to the processes (1) or (2). The decision to start with only two pathway (fast

and slow) was based on a preliminary analysis of the comet data from melanoma and sarcoma (data not shown): The time resolved amount of DNA-fragments in the comet tail exhibits 1-2 shoulders indicating two different pathways with different repair speed. In Fig 4, a flow chart for the 2-pathway model is shown: DNA damages (number n_0; including SSB and DSB) are produced with an induction rate proportional to the dose rate R ($dn_0 / dt = k_{cleav} R$; k_{cleav} is a cleavage constant). Since there is a large number of remaining potential target sites (DNA fragments in tail typically below 25%), it is assumed that there is no saturation effect. It has to be pointed out here that this is a simplistic approach for fragment generation. Since a fragment will be cut out of a DNA strand by 2 hits, one would expect an additional dependence of the absorbed dose D at the corresponding time t: $dn_0 / dt = k_{cleav} R \cdot D$. In addition, pre-existing, non-radiation induced breaks can lead to the liberation of a fragment, when a second, radiation-induced break will occur. This process is then, as initially assumed, simply proportional to the dose rate. Both possibilities combined will yield: $dn_0 / dt = k_{cleav} R \cdot (\varepsilon - D)$, where ε is a dose-equivalent for pre-existing, not-radiation induced breaks. Simulations with the different models and varying parameter values for ε resulted only in different values for k_{cleav} without significant impact on the terminal course of the number of fragments in the tail. Since the number of data points is limited and experiments were performed at only one dose rate, we decided to use the simplest approach for fragment generation in this study.

Figure 4: Process flow chart for the 2-pathway model. Primary damages (n_0) are detected by one of the two repair pathways and then transformed to damages prepared for the fast ($n_{1,fast}$) or slow ($n_{1,slow}$) pathway (by a first order kinetics). The damages are further processed and prepared for end-joining (or in case of HR, homology search). Processed DNA fragments

($n_{2,fast}$ and $n_{2,slow}$) fade away by the final repair step (second order kinetics). The full set of equations of the mathematical model is given in additional file 1.

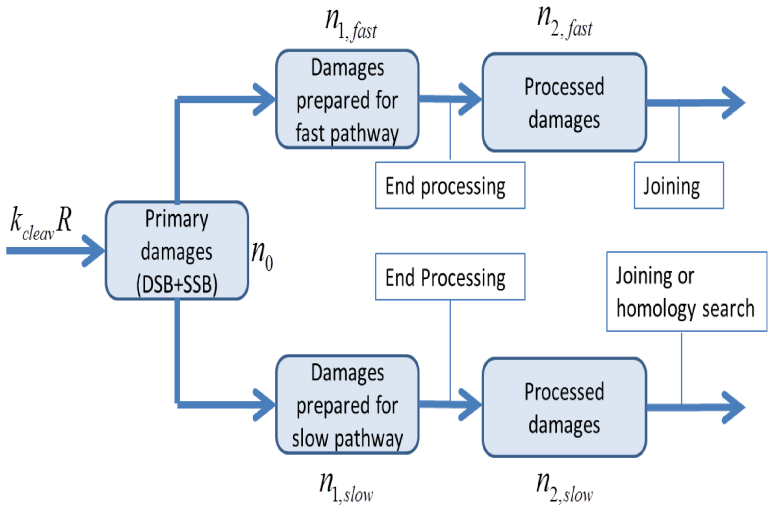

The primary damages (n_0) can be detected by one of the two repair pathways and then transformed to damages prepared for the fast ($n_{1,fast}$) or the slow ($n_{1,slow}$) pathway. For this process, first order kinetics is assumed. After detection by a repair-pathway, the damages will be processed and prepared for end-joining (or in case of HR, homology search). The amount (number) of processed damages is denoted by $n_{2,fast}$ and $n_{2,slow}$ respectively. It is further assumed that all types of damages (n_0, $n_{1,fast}$, $n_{1,slow}$, $n_{2,fast}$, $n_{2,slow}$) can be transported by electrophoresis and are therefore visible in the comet tail. Free DNA fragments fade away by the final repair process step, which is described by second order kinetics in the model since two fragments are joint together. The full set of equations of the mathematical model and parameter values is given in additional file 1.

For the model-based analysis, the median values of % DNA fragments in comet tail have been calculated. To determine the parameter values in the model, an evolutionary optimization algorithm using a gradient search method was applied [39].

Statistical methods

Data were coded in Excel and analyzed with SPSS version 21. Descriptive statistics such as means, standard deviations, medians, interquartile ranges (IQR) together with corresponding 95% confidence intervals (95% CI) were computed. The non-parametric Spearman correlations for associations between two continuous variables were computed. Due to the time dependence a linear mixed model approach was applied to detect associations between the comet median tail intensity in % (0, 15, 30, 60, 120, 360 minutes after RT and compared to the beginning of the next fraction), median γH2AX positive stained cells in %, median number of γH2AX foci per cell (0, 30, 360 minutes after RT and compared to the beginning of the next fraction) adjusted for the following predictors: age, gender, tumor volume and histological group.

For the analysis of the baseline levels of γH2AX in tumor biopsy samples of various histologies the Kolmogorov-Smirnov test was applied to check the correctness of normality assumption of the median γH2AX positive stained cells in % and median number of γH2AX foci per cell. The one-way ANOVA together with the Scheffé post-hoc test approach was taken to investigate differences in primary outcomes of median γH2AX positive stained cells in % and median number of γH2AX foci in the nucleus, age and weight with respect to diagnostic code. The association between the diagnostic code and gender was checked with the Chi^2-test.

Results of statistical analysis with p-value <5% were interpreted as statistically significant.

Ethics approval and consent to participate

This study was carried out in strict accordance with the recommendations and the protocol approved by the Animal Ethics Council of the Canton of Zurich, Switzerland (permit numbers: 180/2011 and ZH108/15), which included owners' consent.

Competing interests

The authors declare that they have no competing interests.

Funding

Marie-Louise von Muralt-Stiftung für Kleintiere, Zurich, Switzerland - Prof. Carla Rohrer Bley

Krebsliga Zurich, Switzerland - Prof. Carla Rohrer Bley

Swiss Life Jubilee foundation, Zurich - Dr. Hassan Chaachouay

Schweizerischer Nationalfonds zur Förderung der Wissenschaftlichen Forschung (320030_163435) - Prof. Stephan Scheidegger

Author's contributions

NS, KNK, SSC, and CRB wrote the manuscript. NS and CRB enrolled the patients and collected the samples. NS, HCH, FG, MR and SSC analyzed the data. SSC and CRB conceived of the study, participated in its design and coordination. All authors contributed to and approved the final version of the manuscript.

Acknowledgements

none

References

1. Koch, U.; Hohne, K.; von Neubeck, C.; Thames, H.D.; Yaromina, A.; Dahm-Daphi, J.; Baumann, M.; Krause, M. Residual gammah2ax foci predict local tumour control after radiotherapy. *Radiotherapy and oncology : journal of the European Society for Therapeutic Radiology and Oncology* **2013**, *108*, 434-439.

2. Menegakis, A.; De Colle, C.; Yaromina, A.; Hennenlotter, J.; Stenzl, A.; Scharpf, M.; Fend, F.; Noell, S.; Tatagiba, M.; Brucker, S.*, et al.* Residual gammah2ax foci after ex vivo irradiation of patient samples with known tumour-type specific differences in radio-responsiveness. *Radiotherapy and oncology : journal of the European Society for Therapeutic Radiology and Oncology* **2015**, *116*, 480-485.

3. Menegakis, A.; Yaromina, A.; Eicheler, W.; Dorfler, A.; Beuthien-Baumann, B.; Thames, H.D.; Baumann, M.; Krause, M. Prediction of clonogenic cell survival curves based on the number of residual DNA double strand breaks measured by gammah2ax staining. *Int J Radiat Biol* **2009**, *85*, 1032-1041.

4. Wouters, B.G.; Begg, A.C. Irradiation-induced damage and the DNA damage response. In *Basic clinical radiobiology*, 4th ed.; Joiner M, V.d.K.A., Ed. Arnold: Great Britain, 2009; pp 11-26.

5. Menegakis, A.; von Neubeck, C.; Yaromina, A.; Thames, H.; Hering, S.; Hennenlotter, J.; Scharpf, M.; Noell, S.; Krause, M.; Zips, D.*, et al.* Gammah2ax assay in ex vivo irradiated tumour specimens: A novel method to determine tumour radiation sensitivity in patient-derived material. *Radiotherapy and oncology : journal of the European Society for Therapeutic Radiology and Oncology* **2015**, *116*, 473-479.

6. Bowman, K.J.; Al-Moneef, M.M.; Sherwood, B.T.; Colquhoun, A.J.; Goddard, J.C.; Griffiths, T.R.; Payne, D.; Singh, S.; Butterworth, P.C.; Khan, M.A.*, et al.* Comet assay measures of DNA damage are predictive of bladder cancer cell treatment sensitivity in

vitro and outcome in vivo. *International journal of cancer. Journal international du cancer* **2014**, *134*, 1102-1111.

7. Lord, C.J.; Ashworth, A. Bringing DNA repair in tumors into focus. *Clinical cancer research : an official journal of the American Association for Cancer Research* **2009**, *15*, 3241-3243.

8. Graeser, M.; McCarthy, A.; Lord, C.J.; Savage, K.; Hills, M.; Salter, J.; Orr, N.; Parton, M.; Smith, I.E.; Reis-Filho, J.S.*, et al.* A marker of homologous recombination predicts pathologic complete response to neoadjuvant chemotherapy in primary breast cancer. *Clinical cancer research : an official journal of the American Association for Cancer Research* **2010**, *16*, 6159-6168.

9. Li, W.; Li, F.; Huang, Q.; Shen, J.; Wolf, F.; He, Y.; Liu, X.; Hu, Y.A.; Bedford, J.S.; Li, C.Y. Quantitative, noninvasive imaging of radiation-induced DNA double-strand breaks in vivo. *Cancer Res* **2011**, *71*, 4130-4137.

10. Somaiah, N.; Yarnold, J.; Daley, F.; Pearson, A.; Gothard, L.; Rothkamm, K.; Helleday, T. The relationship between homologous recombination repair and the sensitivity of human epidermis to the size of daily doses over a 5-week course of breast radiotherapy. *Clinical cancer research : an official journal of the American Association for Cancer Research* **2012**, *18*, 5479-5488.

11. Collins, A.R. The comet assay for DNA damage and repair: Principles, applications, and limitations. *Mol Biotechnol* **2004**, *26*, 249-261.

12. Fikrova, P.; Stetina, R.; Hronek, M.; Hyspler, R.; Ticha, A.; Zadak, Z. Application of the comet assay method in clinical studies. *Wien Klin Wochenschr* **2011**, *123*, 693-699.

13. McKenna, D.J.; McKeown, S.R.; McKelvey-Martin, V.J. Potential use of the comet assay in the clinical management of cancer. *Mutagenesis* **2008**, *23*, 183-190.

14. Banath, J.P.; Olive, P.L. Expression of phosphorylated histone h2ax as a surrogate of cell killing by drugs that create DNA double-strand breaks. *Cancer Res* **2003**, *63*, 4347-4350.

15. Grosse, N.; van Loon, B.; Rohrer Bley, C. DNA damage response and DNA repair - dog as a model? *BMC cancer* **2014**, *14*, 203.

16. Khanna, C.; Lindblad-Toh, K.; Vail, D.; London, C.; Bergman, P.; Barber, L.; Breen, M.; Kitchell, B.; McNeil, E.; Modiano, J.F.*, et al.* The dog as a cancer model. *Nat Biotechnol* **2006**, *24*, 1065-1066.

17. Park, S.H.; Kang, H.J.; Kim, H.S.; Kim, M.J.; Heo, J.I.; Kim, J.H.; Kho, Y.J.; Kim, S.C.; Kim, J.; Park, J.B.*, et al.* Higher DNA repair activity is related with longer replicative life span in mammalian embryonic fibroblast cells. *Biogerontology* **2011**, *12*, 565-579.

18. Strom, T.; Hoffe, S.E.; Fulp, W.; Frakes, J.; Coppola, D.; Springett, G.M.; Malafa, M.P.; Harris, C.L.; Eschrich, S.A.; Torres-Roca, J.F.*, et al.* Radiosensitivity index predicts for survival with adjuvant radiation in resectable pancreatic cancer. *Radiotherapy and oncology : journal of the European Society for Therapeutic Radiology and Oncology* **2015**, *117*, 159-164.

19. McKeown, S.R.; Robson, T.; Price, M.E.; Ho, E.T.; Hirst, D.G.; McKelvey-Martin, V.J. Potential use of the alkaline comet assay as a predictor of bladder tumour response to radiation. *Br J Cancer* **2003**, *89*, 2264-2270.

20. Moneef, M.A.; Sherwood, B.T.; Bowman, K.J.; Kockelbergh, R.C.; Symonds, R.P.; Steward, W.P.; Mellon, J.K.; Jones, G.D. Measurements using the alkaline comet assay predict bladder cancer cell radiosensitivity. *Br J Cancer* **2003**, *89*, 2271-2276.

21. Collins, A.R.; Dobson, V.L.; Dusinska, M.; Kennedy, G.; Stetina, R. The comet assay: What can it really tell us? *Mutat Res* **1997**, *375*, 183-193.

22. Klaude, M.; Eriksson, S.; Nygren, J.; Ahnstrom, G. The comet assay: Mechanisms and technical considerations. *Mutat Res* **1996**, *363*, 89-96.

23. Olive, P.L. The role of DNA single- and double-strand breaks in cell killing by ionizing radiation. *Radiat Res* **1998**, *150*, S42-51.

24. Dunne, A.L.; Price, M.E.; Mothersill, C.; McKeown, S.R.; Robson, T.; Hirst, D.G. Relationship between clonogenic radiosensitivity, radiation-induced apoptosis and DNA damage/repair in human colon cancer cells. *Br J Cancer* **2003**, *89*, 2277-2283.

25. Bonner, W.M.; Redon, C.E.; Dickey, J.S.; Nakamura, A.J.; Sedelnikova, O.A.; Solier, S.; Pommier, Y. Gammah2ax and cancer. *Nat Rev Cancer* **2008**, *8*, 957-967.

26. Rogakou, E.P.; Boon, C.; Redon, C.; Bonner, W.M. Megabase chromatin domains involved in DNA double-strand breaks in vivo. *J Cell Biol* **1999**, *146*, 905-916.

27. Mirzayans, R.; Severin, D.; Murray, D. Relationship between DNA double-strand break rejoining and cell survival after exposure to ionizing radiation in human fibroblast strains with differing atm/p53 status: Implications for evaluation of clinical radiosensitivity. *Int J Radiat Oncol Biol Phys* **2006**, *66*, 1498-1505.

28. Derenzini, E.; Agostinelli, C.; Imbrogno, E.; Iacobucci, I.; Casadei, B.; Brighenti, E.; Righi, S.; Fuligni, F.; Ghelli Luserna Di Rora, A.; Ferrari, A.*, et al.* Constitutive activation of the DNA damage response pathway as a novel therapeutic target in diffuse large b-cell lymphoma. *Oncotarget* **2015**, *6*, 6553-6569.

29. Fontana, A.O.; Augsburger, M.A.; Grosse, N.; Guckenberger, M.; Lomax, A.J.; Sartori, A.A.; Pruschy, M.N. Differential DNA repair pathway choice in cancer cells after proton- and photon-irradiation. *Radiotherapy and oncology : journal of the European Society for Therapeutic Radiology and Oncology* **2015**, *116*, 374-380.

30. Maeda, J.; Froning, C.E.; Brents, C.A.; Rose, B.J.; Thamm, D.H.; Kato, T.A. Intrinsic radiosensitivity and cellular characterization of 27 canine cancer cell lines. *PloS one* **2016**, *11*, e0156689.

31. Mariotti, L.G.; Pirovano, G.; Savage, K.I.; Ghita, M.; Ottolenghi, A.; Prise, K.M.; Schettino, G. Use of the gamma-h2ax assay to investigate DNA repair dynamics following multiple radiation exposures. *PloS one* **2013**, *8*, e79541.

32. Menegakis, A.; Eicheler, W.; Yaromina, A.; Thames, H.D.; Krause, M.; Baumann, M. Residual DNA double strand breaks in perfused but not in unperfused areas determine different radiosensitivity of tumours. *Radiotherapy and oncology : journal of the European Society for Therapeutic Radiology and Oncology* **2011**, *100*, 137-144.

33. Paris, L.; Cordelli, E.; Eleuteri, P.; Grollino, M.G.; Pasquali, E.; Ranaldi, R.; Meschini, R.; Pacchierotti, F. Kinetics of gamma-h2ax induction and removal in bone marrow and testicular cells of mice after x-ray irradiation. *Mutagenesis* **2011**, *26*, 563-572.

34. Olive, P.L.; Banath, J.P. Phosphorylation of histone h2ax as a measure of radiosensitivity. *Int J Radiat Oncol Biol Phys* **2004**, *58*, 331-335.

35. Rube, C.E.; Grudzenski, S.; Kuhne, M.; Dong, X.; Rief, N.; Lobrich, M.; Rube, C. DNA double-strand break repair of blood lymphocytes and normal tissues analysed in a preclinical mouse model: Implications for radiosensitivity testing. *Clinical cancer research : an official journal of the American Association for Cancer Research* **2008**, *14*, 6546-6555.

36. Sedelnikova, O.A.; Bonner, W.M. Gammah2ax in cancer cells: A potential biomarker for cancer diagnostics, prediction and recurrence. *Cell Cycle* **2006**, *5*, 2909-2913.

37. Novik, K.L.; Spinelli, J.J.; Macarthur, A.C.; Shumansky, K.; Sipahimalani, P.; Leach, S.; Lai, A.; Connors, J.M.; Gascoyne, R.D.; Gallagher, R.P.*, et al.* Genetic variation in h2afx

contributes to risk of non-hodgkin lymphoma. *Cancer Epidemiol Biomarkers Prev* **2007**, *16*, 1098-1106.

38. Bodgi, L.; Foray, N. The nucleo-shuttling of the atm protein as a basis for a novel theory of radiation response: Resolution of the linear-quadratic model. *Int J Radiat Biol* **2016**, *92*, 117-131.

39. Scheidegger, S.; Fuchs, H.U.; Zaugg, K.; Bodis, S.; Fuchslin, R.M. Using state variables to model the response of tumour cells to radiation and heat: A novel multi-hit-repair approach. *Computational and mathematical methods in medicine* **2013**, *2013*, 587543.

40. Yu, Y.; Zhu, W.; Diao, H.; Zhou, C.; Chen, F.F.; Yang, J. A comparative study of using comet assay and gammah2ax foci formation in the detection of n-methyl-n'-nitro-n-nitrosoguanidine-induced DNA damage. *Toxicol In Vitro* **2006**, *20*, 959-965.

41. Begg, A.C. Predicting response to radiotherapy: Evolutions and revolutions. *Int J Radiat Biol* **2009**, *85*, 825-836.

42. Torres-Roca, J.F.; Stevens, C.W. Predicting response to clinical radiotherapy: Past, present, and future directions. *Cancer Control* **2008**, *15*, 151-156.

43. Olive, P.L.; Banath, J.P. The comet assay: A method to measure DNA damage in individual cells. *Nat Protoc* **2006**, *1*, 23-29.

44. Qvarnstrom, O.F.; Simonsson, M.; Johansson, K.A.; Nyman, J.; Turesson, I. DNA double strand break quantification in skin biopsies. *Radiotherapy and oncology : journal of the European Society for Therapeutic Radiology and Oncology* **2004**, *72*, 311-317.

45. Rogakou, E.P.; Pilch, D.R.; Orr, A.H.; Ivanova, V.S.; Bonner, W.M. DNA double-stranded breaks induce histone h2ax phosphorylation on serine 139. *The Journal of biological chemistry* **1998**, *273*, 5858-5868.

46. MacNeill, A.L. Cytology of canine and feline cutaneous and subcutaneous lesions and lymph nodes. *Top Companion Anim Med* **2011**, *26*, 62-76.

47. Cancedda, S.; Marconato, L.; Meier, V.; Laganga, P.; Roos, M.; Leone, V.F.; Rossi, F.; Rohrer Bley, C. Hypofractionated radiotherapy for macroscopic canine soft tissue sarcoma: A retrospective study of 50 cases treated with a 5 x 6 gy protocol with or without metronomic chemotherapy *Vet Radiol Ultrasound* **2015**.

48. Keyerleber, M.A.; McEntee, M.C.; Farrelly, J.; Podgorsak, M. Completeness of reporting of radiation therapy planning, dose, and delivery in veterinary radiation oncology manuscripts from 2005 to 2010. *Vet Radiol Ultrasound* **2012**, *53*, 221-230.

49. Rohrer Bley, C.; Blattmann, H.; Roos, M.; Sumova, A.; Kaser-Hotz, B. Assessment of a radiotherapy patient immobilization device using single plane port radiographs and a remote computed tomography scanner. *Vet Radiol Ultrasound* **2003**, *44*, 470-475.

50. Iliakis, G.; Wu, W.; Wang, M. DNA double strand break repair inhibition as a cause of heat radiosensitization: Re-evaluation considering backup pathways of nhej. *International journal of hyperthermia : the official journal of European Society for Hyperthermic Oncology, North American Hyperthermia Group* **2008**, *24*, 17-29.

Supporting Information

Additional File 1: Bio-mathematical 2-pathway model. The initial number of fragments $n_0 = n_0(t)$ is assumed to be produced proportional to the dose rate *R* and a cleavage constant k_{cleav}. The number of fragments $n_{1,fast} = n_{1,fast}(t)$ represents fragments recruited for the fast repair-pathway by a first order kinetics process with the speed constant $k_{0,fast}$. Following the fast repair pathway, the number $n_{2,fast} = n_{2,fast}(t)$ is counting fragments prepared for the fast final repair process by a "delayed" first order kinetics process with the speed constant $k_{1,fast}$, the delay time $t_{r,fast}$. These fragments are removed by a second order process (2 fragments are linked together) with the repair constant $k_{2,fast}$. The slow repair pathway has the same structure with the number of fragments recruited for the slow repair-pathway $n_{1,slow} = n_{1,slow}(t)$ by a first order kinetics process with the speed constant $k_{0,slow}$ and the number of fragments $n_{2,slow} = n_{2,slow}(t)$ prepared for the slow final repair process by a "delayed" first order kinetics process (speed constant $k_{1,slow}$; delay time $t_{r,slow}$) and removed by second order repair (repair constant $k_{2,slow}$). The total number of free fragments (visible in the Comet tail) is calculated by:

$$n_{Comet} = n_0 + \sum_i (n_{i,fast} + n_{i,slow}) + b_n \qquad (1)$$

where b_n is the base line number of fragments that can be estimated along with the other parameters. All numbers of fragments are scaled to the percentage of DNA in tail (%DNA fragments in tail, corresponding to the experimental data). The induction-, production- and

repair rates are given by the following system of ordinary (ODE) and delay differential equations (DDE):

$$\frac{dn_0}{dt} = k_{cleav}R - (k_{0,fast} + k_{0,slow}) \cdot n_0$$

$$\frac{dn_{1,fast}}{dt} = k_{0,fast}n_0 - k_{1,fast}n_{1,fast}(t - t_{r,fast})$$

$$\frac{dn_{2,fast}}{dt} = k_{1,fast}n_{1,fast}(t - t_{r,fast}) - k_{2,fast}n_{2,fast}^2$$

$$\frac{dn_{1,slow}}{dt} = k_{0,slow}n_0 - k_{1,slow}n_{1,slow}(t - t_{r,slow})$$

$$\frac{dn_{2,slow}}{dt} = k_{1,slow}n_{1,slow}(t - t_{r,slow}) - k_{2,slow}n_{2,slow}^2 \qquad (2)$$

With the initial conditions:

$$n_0(0) = n_{2,fast}(0) = n_{2,slow}(0) = 0$$

and

$$n_{1,fast}(t<0) = n_{1,slow}(t<0) = 0$$

Additional File 2: Absolute values of median tail intensity (% DNA in tail), comet assay (%; 95% CI). T_0, T_{15}, T_{30}, etc. indicate the time-points in minutes after completion of radiation treatment

Time-points	% DNA in tail (95% CI)	p-value
T_0	4.31	
T_{15}	15.11 (11.98 – 18.24)	p=0.001
T_{30}	15.55 (12.25 – 18.84)	p=0.001
T_{60}	11.42 (8.79 – 14.04)	p<0.001
T_{120}	6.78 (3.29 – 10.27)	p=0.172
T_{360}	5.55 (3.27 – 7.82)	p=0.185

CURRICULUM VITAE

Vorname Name	Nadine Schulz
Geburtsdatum	23.11.1986
Geburtsort	Oberhausen, Deutschland
Nationalität	deutsch

Schulausbildung

08/1993 - 07/1997	Osterfelder-Heide-Schule, Städt. Gemeinschaftsgrundschule (Oberhausen, DE)
08/1997 - 06/2006	Freiherr-vom-Stein-Gymnasium (Oberhausen, DE)

Höchster Schulabschluss

06/2006	Abitur, Freiherr-vom-Stein-Gymnasium (Oberhausen, DE)

Studium

10/2007 - 06/2014	Diplomstudium Veterinärmedizin Vetmeduni Vienna, Wien, AT
01/2014	Abschlussprüfung Magister med. vet./Diplomtierarzt Vetmeduni Vienna, Wien, AT
03/2014 – 01/2016	Anfertigung der Dissertation unter Leitung von: Prof. Dr. med. vet. Carla Rohrer Bley am Departement für Kleintiere Abteilung Radio-Onkologie der Vetsuisse-Fakultät, Universität Zürich Leitung Prof. Dr. med. vet. Carla Rohrer Bley

Fachrelevante Anstellungen nach Abschluss des veterinärmedizinischen Studiums

März 2014 bis Januar 2016	Doktorandin und Assistenzärztin am Departement für Kleintiere, Abteilung Radio-Onkologie, Vetsuisse Fakultät, Universität Zürich
Februar 2016 bis heute	Tierärztin Tierklinik Neuwied, Neuwied, Deutschland